

## Licença

Autores que publicam nesta revista concordam com os seguintes termos:

- a. Autores mantêm os direitos autorais e concedem à revista o direito de primeira publicação, com o trabalho simultaneamente licenciado sob a Licença Creative Commons Attribution que permite o compartilhamento do trabalho com reconhecimento da autoria e publicação inicial nesta revista.
- b. Autores têm autorização para assumir contratos adicionais separadamente, para distribuição não-exclusiva da versão do trabalho publicada nesta revista (ex.: publicar em repositório institucional ou como capítulo de livro), com reconhecimento de autoria e publicação inicial nesta revista.
- c. Autores têm permissão e são estimulados a publicar e distribuir seu trabalho online (ex.: em repositórios institucionais ou na sua página pessoal) a qualquer ponto antes ou durante o processo editorial, já que isso pode gerar alterações produtivas, bem como aumentar o impacto e a citação do trabalho publicado (Veja O Efeito do Acesso Livre).

### Fonte:

<https://ojs.studiespublicacoes.com.br/ojs/index.php/cadped/article/view/1937>.

Acesso em: 02 jul. 2025.

**Referência:** OLIVEIRA, Thiago Arnaud Abreu *et al.* A new approach for correlating Paris parameters with fatigue life of aircraft fuselage panels. *Caderno Pedagógico*, [S. l.], v. 20, n. 7, p. 2359-2391, 2023. DOI: <https://doi.org/10.54033/cadpedv20n7-001>.

Disponível em:

<https://ojs.studiespublicacoes.com.br/ojs/index.php/cadped/article/view/1937>.

Acesso em: 02 jul. 2025.

## A new approach for correlating Paris parameters with fatigue life of aircraft fuselage panels

## Uma nova abordagem para correlacionar os parâmetros de Paris com a vida à fadiga dos painéis da fuselagem de aeronaves

DOI: 10.54033/cadpedv20n7-001

Recebimento dos originais: 03/11/2023  
Aceitação para publicação: 04/12/2023

---

### Thiago Arnaud Abreu Oliveira

Master in Structures

Institution: Universidade de Brasília - campus Darcy Ribeiro

Address: Campus Universitário Darcy Ribeiro, Asa Norte, Brasília - DF,  
CEP: 70910-900

E-mail: eng.thiagoarnaud@gmail.com

### Gilberto Gomes

Doctor in Structures

Institution: Universidade de Brasília - campus Darcy Ribeiro

Address: Campus Universitário Darcy Ribeiro, Asa Norte, Brasília - DF,  
CEP: 70910-900

E-mail: ggomes@unb.br

### Álvaro Martins Delgado Neto

Master in Structures

Institution: Universidade de Brasília - campus Darcy Ribeiro

Address: Campus Universitário Darcy Ribeiro, Asa Norte, Brasília - DF,  
CEP: 70910-900

E-mail: alvaro.martins.bok@gmail.com

### Iuri Augusto Alves Lustosa

Master in Structures

Institution: Instituto Federal do Piauí (IFPI) - campus Parnaíba

Address: Avenida Monsenhor Antonio Sampaio, s/n, Dirceu Arcoverde,  
Parnaíba – PI, CEP: 64211-145

E-mail: iuri.lustosa@ifpi.edu.br

### Wellington Vital

Doctor in Structures

Institution: Universidade de Brasília - campus Darcy Ribeiro

Address: Campus Universitário Darcy Ribeiro, Asa Norte, Brasília - DF,  
CEP: 70910-900

E-mail: wellington.silva@unb.br

**ABSTRACT**

This work presents a numerical technique that establishes a relationship between the C and m parameters of the Paris Law and the number of fatigue life cycles. This relationship is particularly important for determining the material's ability to withstand a specified number of cycles in an aircraft fuselage design. The methodology is based on a multiscale problem and comprises two stages: the macro model, which focuses on internal stresses and critical point location, and the micro model, which considers the critical fatigue life cycle number (n) across a "grid" of C and m parameters, resulting in the optimal curve  $N(C,m)$ . To validate the adopted methodology, the academic program BemCracker2D has been used to calculate the internal stress fields, simulate cracks, and estimate fatigue life. Three case studies were conducted, and the results indicated that the range of C and m values obtained depends on the configuration of the macro model, the physical parameters of the material, and the defined number of cycles in the design. Ultimately, this computational technique allows for generalization to any fuselage damage analysis model, providing C and m Paris parameter data to mitigate fatigue damage.

**Keywords:** damage tolerance, fatigue life, aircraft fuselage, DBEM, multiscale analysis.

**RESUMO**

Este trabalho apresenta uma técnica numérica que estabelece uma relação entre os parâmetros C e m da Lei de Paris e o número de ciclos de vida em fadiga. Esta relação é particularmente importante para determinar a capacidade do material de suportar um número específico de ciclos no projeto da fuselagem de uma aeronave. A metodologia é baseada em um problema multiescala e compreende duas etapas: o modelo macro, que foca nas tensões internas e localização de pontos críticos, e o modelo micro, que considera o número do ciclo de vida de fadiga crítica (n) através de uma "grade" de C e m parâmetros, resultando na curva ótima  $N(C,m)$ . Para validar a metodologia adotada, foi utilizado o programa acadêmico BemCracker2D para calcular os campos de tensões internas, simular trincas e estimar a vida em fadiga. Foram realizados três estudos de caso e os resultados indicaram que a faixa de valores C e m obtidos depende da configuração do macromodelo, dos parâmetros físicos do material e do número de ciclos definido no projeto. Em última análise, esta técnica computacional permite a generalização para qualquer modelo de análise de danos na fuselagem, fornecendo dados de parâmetros C e m Paris para mitigar os danos por fadiga.

**Palavras-chave:** tolerância a danos, vida em fadiga, fuselagem de aeronave, DBEM, análise multiescala.

## 1 INTRODUCTION

The evaluation of Fracture Mechanics (FM) parameters, such as Stress Intensity Factor (SIF), number of loading cycles, and stress and displacement fields in the aircraft fuselage, is challenging due to the complex nature of panel details, including supports, shear clips, and rivets. However, it is crucial to understand the damage process, especially under dynamic loads. Designers are continuously seeking efficient and dependable simulation methods that can provide precise average data for these parameters in order to prevent damage processes and accidents. In this context, automation plays a vital role in conducting multiple analyses for parametric studies, ultimately leading to design optimization [1].

To address fracture problems, various numerical methods based on domains, such as the Finite Element Method (FEM), Extended Finite Element Method (XFEM), and Generalized Finite Element Method (GFEM), as well as boundary-based methods like the Boundary Element Method (BEM) and Dual Boundary Element Method (DBEM), are gaining popularity. Among these methods, DBEM offers several advantages. It simplifies the modeling of the crack area, directly calculates the Stress Intensity Factor (SIF), reduces execution times, and accurately simulates crack growth [2]–[4]. By discretizing only the boundaries of a solid, DBEM enables the analysis of thousands of simulations necessary for probabilistic studies. Furthermore, DBEM can be utilized to study defects, predict fatigue behavior, analyze the damage process, evaluate multiple site damages, and assess reliability [5]–[9].

There are several numerical simulation programs for structural modeling and analysis, with Abaqus and ANSYS being two of the most popular options for Finite Element Method (FEM). Additionally, FRANC 3D is a numerical simulation program specifically designed for Boundary Element Method analysis (BEM). In addition to these, there are notable home-made software tools such as BemLab and BemCracker2D, which have been prominently used in several scientific works, including references [10]–[13]. For the technique developed in this work, the use of these programs is crucial, starting from the modeling stage, through processing, and finally for result analysis. The objective of developing this tool is

to automate the entire process of defining Paris parameters, thereby assisting in material selection.

This work aims to introduce a computational tool that utilizes the Boundary Element Method (BEM) to assess two-dimensional aircraft fuselage models. The tool generates an optimized function for the Paris parameters, which can support a specified number of fatigue life cycles determined by the designer. The process involves the designer creating a macro model and specifying the desired number of cycles. The automated tool then processes the model, evaluates the C and m Paris parameters required to withstand the specified number of cycles, and provides an optimized function accordingly. In essence, this paper serves as a continuation of the previous works conducted in references [11]–[13]. It builds upon the research conducted in those works to develop and present an advanced computational tool that enables the evaluation and optimization of Paris parameters for aircraft fuselage models using BEM.

This paper is structured as follows: Section 2 briefly reviews the Evolving Research Trajectory: Insights and innovations over time; Section 3 provides an overview of the current state of the art regarding the fatigue history of aircraft fuselage panels; Section 4 outlines the methodology and the procedure employed in this study. It describes the techniques and tools used for the evaluation and optimization of fatigue parameters in aircraft fuselage models; In Section 5, a model example is shown to validate the application of the methodology used; Section 6 presents the results and discussion obtained from the analysis of three case studies; Finally, Section 7 offers the conclusions drawn from the results and the technique presented in this paper.

## 2 EVOLVING RESEARCH TRAJECTORY

Crack propagation and its implications on material stability have long been subjects of intense scientific investigation. Over the course of a series of interconnected studies, our research journey has traversed through distinct phases, each building upon the insights of its predecessor. In this article, we present a comprehensive overview of this progressive exploration, culminating in our

current work that aspires to bridge theoretical understanding with practical applications.

The foundational stone of our inquiry was laid in the first phase [11], where we challenged the conventional viewpoint that defined instability solely by crack size. Through rigorous analysis and inventive perspectives, we uncovered a pivotal shift — compliance, rather than crack size, emerged as a paramount indicator. We observed that compliance surges towards infinity upon reaching a critical value of  $3C$ , with the number of cycles at this juncture serving as the decisive parameter. A novel analytical calculation for the stress field augmented these revelations. However, the complexity introduced by evaluating thousands of combinations involving random variables necessitated a cautious interpretation.

Expanding our scope, the second phase saw our investigation extend to various materials [12]. By dissecting the growth rates of cracks across diverse metallic alloys, we unveiled correlations between fracture properties and these propagation rates. Our efforts bore fruit with the identification of the lower and upper limits of instability curves, adding a quantifiable dimension to our explorations. Moreover, this phase's conclusions were constrained by the specificity of materials under examination.

In our third phase [13], the focus shifted to numerical simulations. We endeavored to bridge theory and practice, validating its predictions against empirical data. This step forward, coupled with the direct calculation of stress fields via the Boundary Element Method (BEM), fortified our analytical arsenal. Although initially constrained to a specific model, this phase paved the way for future endeavors.

Building upon the insights accrued through this evolutionary journey, our current work emerges as a synthesis of cumulative knowledge. By reintroducing certain parameters as random variables, we aim to identify the most critical combinations yielding worst-case scenarios. Our approach transcends specific models, achieving a level of generalization essential for real-world applicability. It is important to acknowledge the limitations that underpinned our prior research, meticulously considered as we strive to strike a balance between flexibility and precision. In this respect, and in a summarized way, we delve into the intricacies of

each phase, revealing the contributions, limitations and innovations of our research trajectory, as seen in the chart below.

Board 1 - Research trajectory: papers [11, 12 and 13] and current

[11]	[12]	[13]	[Current]
<ul style="list-style-type: none"> <li>✓ Compliance is assessed as the defining variable for instability instead of crack size.</li> <li>✓ Discovery that compliance already tends to infinity upon reaching the value of <math>3C</math>, with the number of cycles at this point being critical.</li> <li>✓ Analytical calculation of the stress field.</li> <li>✓ Evaluation of a thousand combinations with random variables <math>P</math>, <math>Q</math>, <math>R</math>, <math>L1</math>, <math>L2</math>, <math>C</math>, <math>m</math>.</li> <li>✓ Discovery of the critical position for that specific case.</li> </ul>	<ul style="list-style-type: none"> <li>✓ Discovery of the minimum and maximum limits of instability curves.</li> </ul>	<ul style="list-style-type: none"> <li>✓ First attempt to relate Paris' <math>C, m</math> with fatigue life using this method.</li> <li>✓ Direct calculation of stress field through the BEM.</li> <li>✓ Limited application solely to the first model [11] for validation of the stress field.</li> <li>✓ The numerical stress field enables generalization to any case.</li> <li>✓ Evaluation constrained to a single combination of <math>R</math>, <math>L1</math>, <math>L2</math>, as assessment of singular values of this parameter does not reveal the worst-case scenario.</li> </ul>	<ul style="list-style-type: none"> <li>✓ Reintroduction of <math>R</math>, <math>L1</math>, <math>L2</math> as random variables, allowing identification of the combination yielding the worst-case scenario.</li> <li>✓ Application now becomes fully generalized for various models, as per the designer's requirements.</li> </ul>

Source: The authors (2023)

### 3 LITERATURE REVIEW

In recent papers, there is a series of fatigue studies on structural elements. Among them, the works [14]–[17] stand out. Ma [14] examined fatigue life prediction in automobile components. In this work, multiaxial random fatigue damage was adopted to predict the fatigue life of half-shaft and the results show that the prediction method is reliable and meets the service life and safety requirements. Zhang [15] presented a power exponential fatigue equivalent damage model capable of describing the residual strength degradation of materials to improve the fatigue life predictions, considering that when the loading sequence of fatigue loads changes, the fatigue cumulative damage prediction tends to present a large error. Liu [16] improved the accuracy of parameter prediction for small-sample data, considering the existence of error in samples, the error circle was

introduced to analyze original samples. The author discovered that the S-N curve obtained by the error circle method is more reliable; the S-N curve of the Bootstrap method is more reliable than that of the Maximum Likelihood Estimation (MLE) method. Li [17] improved fatigue life analysis method for optimal design of electric multiple units (EMU) gear, which aims at defects of traditional Miner fatigue cumulative damage theory. The results show that it is more corresponded to engineering practice by using the improved fatigue life analysis method than the traditional method.

Similarly, to approximate the Paris law to the material used in aircraft fuselage, Breitbarth [18] investigated fatigue crack growth in sheets of aluminum alloy AA2024-T3 under high-stress conditions. In this experiment, high-stress intensity factors cause plastic zone sizes that extend up to approximately 100 mm from the crack tip. The  $da/dN-\Delta K$  data obtained in this study provide crucial information about the fatigue crack growth and damage tolerance of very long cracks under high-stress conditions in thin lightweight structures.

Still applying these concepts, Toor [19], [20] discussed the requirements for designing a fail-safe fuselage structure for aircraft. It highlights the importance of light weight and high operating stresses for an efficient structural component that must perform its intended function, have a long service life, and be produced at a reasonable cost.

Regarding the damage tolerance, Sayar [21] presented a two-stage fatigue life evaluation of a stiffened aluminium aircraft fuselage panel with a bulging circumferential crack and a broken stringer. In this work, the authors concluded that bulging of the skin due to the internal pressure can have significant effect on the stress intensity factor, resulting in fast crack propagation after the stringer is completely broken. Bakuckas Jr. [22] showed the potential for advanced fuselage panels with varying emerging metallic structures technologies (EMST) to have improved fatigue and damage-tolerance performance compared to panels constructed using conventional materials and fabrication processes. Abdi [23] described a new analysis approach for evaluating the durability and damage tolerance of exterior aircraft attachment installations, which involves considering multiple crack interactions. The analysis was used to evaluate the fatigue crack



initiation and propagation in the fuselage skin and doublers made of wrought aluminum alloys. The results showed that the fatigue damage state in the components at the designed operational life will not exceed the static safety requirements, and therefore, the FAA accepted the damage tolerance analysis.

About the use of computational analysis, Carta [24] validated a numerical method of analysis for predicting the damage tolerance of reinforced panels found in aircraft fuselage. The study uses a fracture mechanics approach with several models simulated with the finite element solver ABAQUS to determine fatigue crack growth rates. The results showed that different solutions for improving the damage tolerance of aircraft reinforced panels can be tested virtually before performing experiments. Proppe [25] presented a probabilistic framework for computing the failure probability of aircraft structural elements under the concept of damage tolerance, which requires the aircraft to have sufficient residual strength in the presence of damage during service inspections. The problem of multi-site damage (MSD) is considered, and uncertainties in crack initiation, crack growth, yield stress, and fracture toughness are described by random variables. The finite element alternating method (FEAM) was used for crack growth calculations, and importance sampling is employed to obtain the probability of failure due to MSD. Kennedy [26] developed a computational technique to predict failure loads in composite structures with through-the-thickness cracks. The discrete crack model with a finite element program was used to simulate damage growth and predict failure over a range of crack sizes. The technique was applied to two laminates and a composite aircraft fuselage, and the results showed good agreement with experimental tests.

Madhavi [27] investigated the damage tolerance design of a transport aircraft fuselage structure, which is subjected to high internal pressurization during each take-off and landing cycle leading to metal fatigue. The study focused on the stress intensity factor for a longitudinal crack under pressurization load and investigates crack initiation, growth, fast fracture, and crack arrest features in the stiffened panel. The analysis was performed using the MSC NASTRAN solver and pre-processed using MSC PATRAN software in order to prevent further crack propagation.

In the upcoming section, the methodology of the proposed technique for damage tolerance in aircraft fuselage is presented. This methodology has been developed based on the extensive analysis conducted to understand the state of the art and specific contributions in this field.

#### 4 MATERIAL AND METHOD

In this section, a computational technique for optimizing the fatigue life of aircraft fuselage parts using compliance is presented. This technique builds upon the previous works published in [11]–[13] and introduces several innovations:

1. The initial defects (R, L1, and L2) are once again considered as random variables, with the same values as presented in the first paper [11]. By evaluating thousands of interactions with different defect sizes, the damage tolerance can be assessed for the worst-case scenario of initial defects;
2. The C and m Paris parameters are optimized to identify the values that can withstand the specified number of cycles defined in the design;
3. The technique creates an optimized function that aids in material selection for aircraft fuselage design.

To accomplish this, the developed technique utilizes an algorithm, named *BLBC\_Algor*, that integrates the BemLab and BemCracker2D software tools, whose idea is the following:

- The designer creates a macro model in BemLab and defines the desired number of cycles ( $n^*$ ).
- BemCracker2D computes the internal stress field in the macro analysis and identifies the stress peak before reaching yielding, allowing for elastic analysis.
- The algorithm positions the micro element at this stress peak and calculates the number of cycles required for compliance to reach 3C ( $N_{3C}$ ).
- Considering a range of initial defects in the micro model (R, L1, L2), the algorithm determines the values of the material's physical parameters (C and m) that result in the minimum number of cycles ( $N_{3C}$ ) reaching the user-defined value ( $n^*$ ).

- Finally, an objective function is derived, which establishes the relationship between the physical parameters of the material (C and m) that ensure the desired number of cycles for the entire plate, ensuring structural integrity.

#### 4.1 BLBC\_ALGOR

1. **Input:** *The designer provides the macro model and specifies the desired number of cycles for fatigue life ( $n^*$ ).*
2. **Random Generation of Initial Defects:** *The algorithm generates random values for the initial defect parameters (R, L1, and L2) based on their predefined range.*
3. **BEM Analysis:** *The Bemcracker2D software is utilized to perform the boundary element analysis, computing the internal stresses field.*
4. **Crack Simulation and Fatigue Life Calculation:** *The BemCracker2D software is employed to simulate crack growth and estimate the fatigue life based on the evaluated initial defects.*
5. **Optimization of Paris Parameters:** *An optimization algorithm is employed to iteratively adjust the C and m values in the Paris Law until the specified number of cycles is achieved.*
6. **Creation of Optimized Function:** *The resulting optimized Paris parameters are used to create a function that assists in material selection for the aircraft fuselage design.*

By following this algorithmic process, the technique enables the optimization of fatigue life for aircraft fuselage parts, considering random initial defects, and provides valuable insights for material selection in the design process.

The objective function holds significant relevance for aircraft designers, as it allows them to determine the appropriate material for a specified number of cycles. For instance, if a designer aims to achieve instability at  $n^*=10^4$  cycles, the optimization process will reveal the specific set of physical parameters (C and m) that the material must possess in order to minimize  $N_{3C}$  and reach the desired number of cycles outlined in the project ( $n^*$ ). By utilizing the objective function,

designers can make informed decisions about material selection, ensuring the structural integrity and safety of the aircraft over the defined lifespan.

## 5 MODEL EXAMPLE

Here is an example model that demonstrates the computational technique described in *BLBC\_Algor* algorithm. The macro model used in this example has already been validated in previous works [11], [13]. The novelty introduced in this paper begins from step 4 onwards.

The technique is divided into two analyses: the macro analysis, which involves designing the model to identify the location of the stress peak (steps 1 and 3), and the micro analysis, which simulates initial damage to determine the critical number of fatigue life cycles (steps 2 and 4). Finally, in steps 5 and 6, an optimized function is developed to relate the Paris parameters to fatigue life. For the sake of simplicity, the steps 1 and 3 can be found in [13] and will not be shown.

According to step 2 of the algorithm, the initial defects of the fuselage (R, L1 and L2) were treated as random variables, with values matching those initially defined in [11] and statistical properties represented in Table 1. These variables followed a lognormal distribution. A total of one thousand combinations of these variables were analyzed. The section 4.2 of the paper will present the results of the analysis, specifically the "Minimum  $N(C,m)$  curve." This curve illustrates the combination of C and m values that yield the minimum number of cycles ( $N_{3C}$ ) required to achieve the user-defined value ( $n^*$ ). By examining this curve, designers will gain insights into the optimized values of C and m that can ensure the desired fatigue life for the fuselage structure.

Table 1 - Statistics of the variables R, L1, and L2

Random variable	Mean	Standard deviation	Coefficient of Variation
R (cm)	0.1	2.0e-02	0.23
L1 (cm)	0.1	1.9e-02	0.22
L2 (cm)	0.1	1.9e-02	0.22

Source: authors (2023)

### 5.1 N(C,M) CURVE

By utilizing the combination of R, L1, and L2 values specified in Table 2, the technique involves varying C and m in a grid form within the domain of  $C = [5e-11, 10e-11]$  and  $m = [2.5, 3.0]$ . This grid-based approach allows for the systematic exploration of different combinations of C and m values.

Table 2 – Example of R, L1, and L2 combination

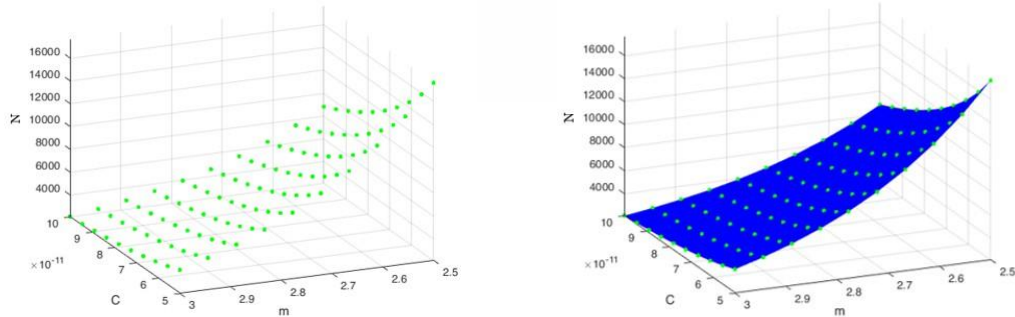
Random variable	Value
R (cm)	0.167
L1 (cm)	0.131
L2 (cm)	0.087

Source: authors (2023)

As a result, the technique generates a set of data points that establish the relationship between C and m values and the corresponding number of cycles. These data points are graphically represented in Figure 1 (a), providing a visual representation of how different values of C and m impact the fatigue life of the fuselage structure. By examining this figure, designers can gain valuable insights into the optimal ranges of C and m that can achieve the desired number of cycles for the given combination of R, L1, and L2 values.

Continuing from Figure 1 (a), the next step involves interpolating the data points to obtain a surface that represents the relationship between C, m, and the number of cycles. This interpolated surface is depicted in Figure 1 (b), providing a visual representation of how C and m values impact the fatigue life of the fuselage structure.

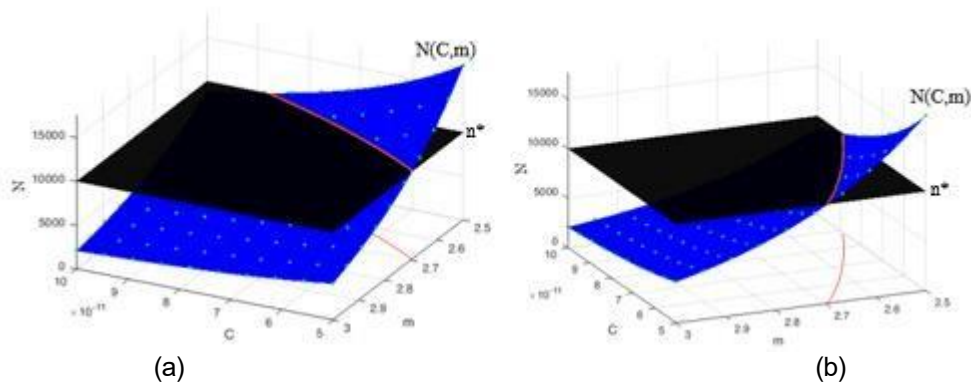
Figure 1 – a) Points of the number of cycles for each combination (C,m); b)  $N(C, m)$  surface.



Source: authors (2023)

To find the values of  $C$  and  $m$  that result in the minimum number of cycles required by the project, one must identify the intersection between the relationship curve and the surface of the desired number of cycles. For example, considering the project's specified number of cycles as  $1e+04$ , the intersection is indicated on the red line in Figure 2 (a). This intersection represents the values of  $C$  and  $m$  that satisfy the fatigue life requirement. Figure 2 (b) displays the curve on the  $C \times m$  plane, indicating the specific values of  $C$  and  $m$  that the material must possess to support the requested number of cycles defined by the user. This curve is also represented in Figure 5 as the  $C$  and  $m$  graph, supporting 10,000 cycles. These visualizations aid in identifying the optimal values of  $C$  and  $m$  for achieving the desired fatigue life of the fuselage structure.

Figure 2 – Intersection between  $N(C,m)$  and the design number of cycles ( $n^*$ )

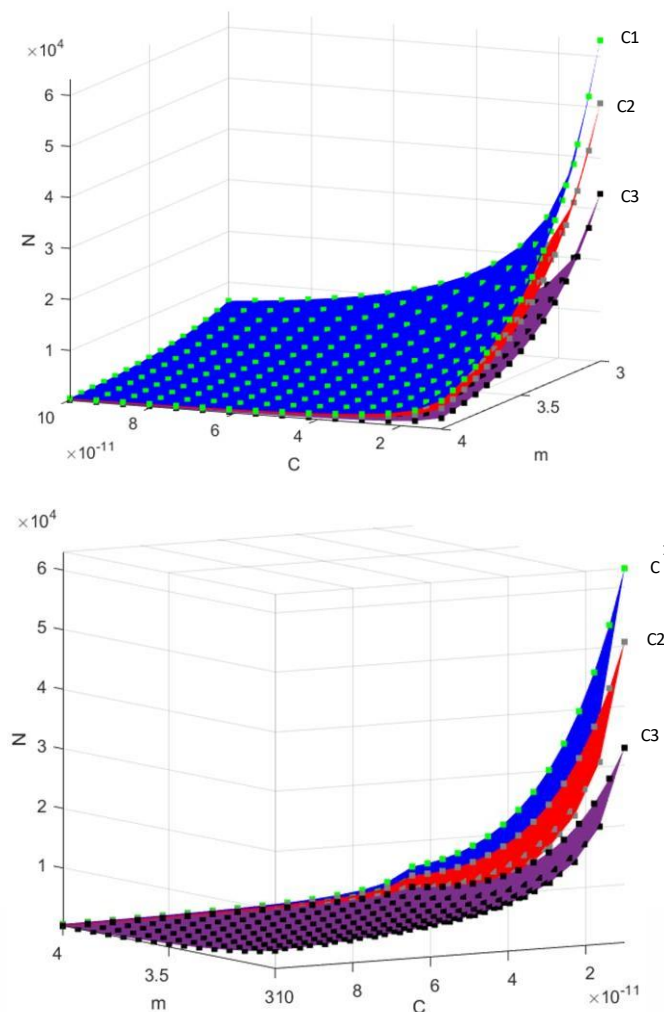


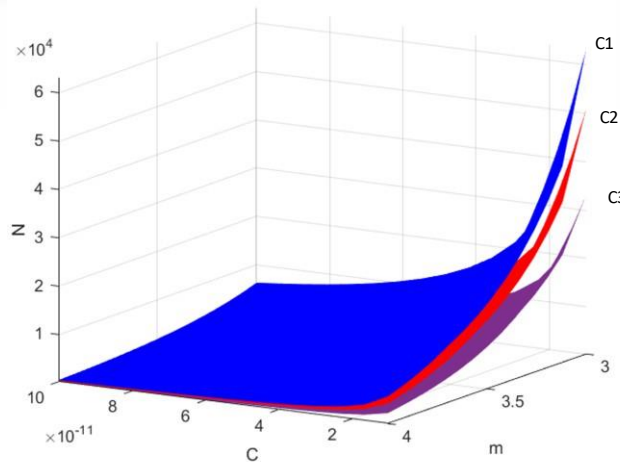
Source: authors (2023)

## 5.2 MINIMUM N(C,M) CURVE

Indeed, it is observed that each combination of initial defects (R, L1, L2) leads to a distinct N(C,m) curve. This characteristic is illustrated in Figure 3, which showcases three examples of combinations (C1, C2, C3) from Table 3. Each combination generates a unique N(C,m) curve, reflecting the influence of the initial defect parameters on the fatigue life of the fuselage structure. The variability in the N(C,m) curves emphasizes the importance of considering different combinations of initial defects in the analysis. It highlights how different defect patterns can impact the relationship between C, m, and the number of cycles, underscoring the need for comprehensive and probabilistic studies to assess the tolerance to damage for various scenarios.

Figure 3 – N(C,m) curves for combinations 1, 2, 3





Source: authors (2023)

Table 3 – Values of R, L1, L2 to combinations 1, 2, 3

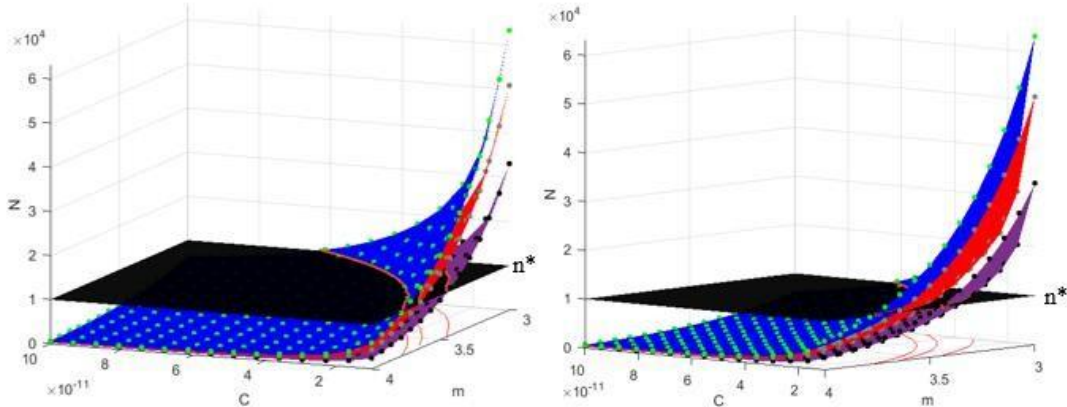
Random variable	Combination 1 (blue curve)	Combination 3 (red curve)	Combination 3 (purple curve)
R (cm)	0.088	0.073	0.086
L1 (cm)	0.111	0.081	0.093
L2 (cm)	0.130	0.105	0.119

Source: authors (2023)

These three curves intersect the desired number of cycles for the design ( $n^*=10^4$ ) at different points, as depicted in Figure 4. The worst-case scenario is represented by the lower curve, as the higher curves can endure a greater number of cycles for the same combination of C and m compared to the lower curve. Consequently, adopting the worst-case scenario is favorable for safety, as it corresponds to the lowest  $N(C,m)$  curve among the thousand combinations analyzed. By considering the worst-case scenario, designers prioritize safety and ensure that the chosen combination of C and m values will support the desired number of cycles, even in the most challenging conditions represented by the lower  $N(C,m)$  curve. This approach accounts for potential variations in initial defect patterns and guarantees the structural integrity and reliability of the fuselage under fatigue loading.



Figure 4 – Different  $N(C,m)$  curves intersections to the number of cycles of project ( $n^*$ )

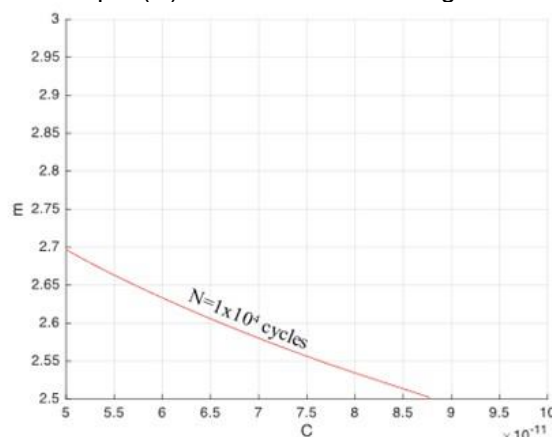


Source: authors (2023)

### 5.3 M(C) CURVE

The lower  $N(C,m)$  curve from the thousand combinations is indeed the minimum  $N(C,m)$  curve. The intersection of this minimum curve with the desired number of cycles ( $n^*$ ), represented by the black surface, results in the  $m(C)$  curve, as depicted in Figure 5. It is important to note that the intersection between the minimum  $N(C,m)$  curve and the black surface (representing the desired number of cycles) corresponds to the optimal values of  $C$  and  $m$  that satisfy the fatigue life requirement. Any other intersections between different  $N(C,m)$  curves and the black surface will be above the  $m(C)$  curve.

Figure 5 – Relationship  $m(C)$  that results in the design number of cycles  $10^4$



Source: authors (2023)

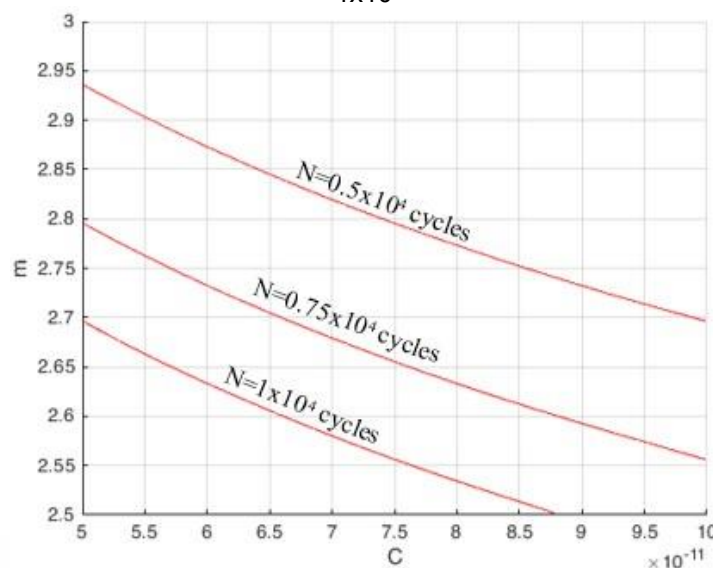
By focusing on the intersection of the minimum  $N(C,m)$  curve and the desired number of cycles, designers can identify the specific values of  $C$  and  $m$  that

the material needs to possess in order to support the requested number of cycles defined by the user. This ensures the selection of appropriate material properties for achieving the desired fatigue life of the fuselage structure.

#### 5.4 VARYING THE DESIGN NUMBER OF CYCLES ( $N^*$ )

Additionally, if the designer wishes to consider a different design number of cycles ( $n^*$ ), the black surface in Figure 2 will shift upwards or downwards, altering the intersection point with the  $N(C,m)$  curve. Consequently, this leads to the movement of the red curve  $m(C)$  within the  $C \times m$  plane, as demonstrated in Figure 6. The vertical movement of the black surface corresponds to a change in the desired number of cycles, and this adjustment influences the selection of the optimal values of  $C$  and  $m$ . As a result, the intersection between the  $N(C,m)$  curve and the black surface will shift accordingly, affecting the position and shape of the red curve  $m(C)$  within the  $C \times m$  plane. Finally, Figure 6 provides a visualization of how the red curve  $m(C)$  changes in response to modifications in the design number of cycles ( $n^*$ ). This understanding enables designers to assess the impact of different fatigue life requirements on the optimal material properties ( $C$  and  $m$ ) for the fuselage structure.

Figure 6 - Relationship  $m(C)$  that results in the design number of cycles  $0.5 \times 10^4$ ,  $0.75 \times 10^4$  e  $1 \times 10^4$



Source: authors (2023)

Finally, there exists an objective function that establishes the relationship between the physical parameters of the material ( $C$  and  $m$ ) and the safe number of cycles for the entire plate. This objective function is represented by the  $m(C)$  curve, which is obtained through a polynomial curve fitting process. The order of the polynomial curve is optimized using the Bayesian Information Criterion (BIC) that is a statistical measure that helps determine the most appropriate model by selecting the one that yields the lowest BIC value, which is given by:

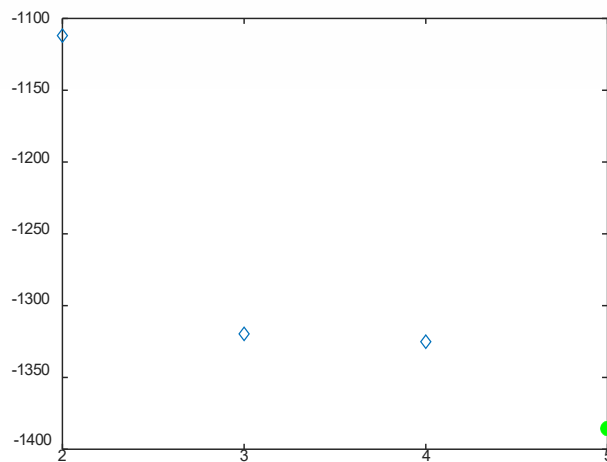
$$BIC = n \ln(\hat{\sigma}_e^2) + k \ln(n) \quad (1)$$

where  $n$  is the number of points,  $\hat{\sigma}_e^2$  is the error variance, and  $k$  the polynomial degree.

In this study, it was observed that a polynomial degree up to 5 was sufficient to accurately represent the intersection curve. The BIC was utilized to identify the minimum BIC value along with the corresponding polynomial degree. The BIC compares different polynomial models with varying degrees to determine the optimal order for the polynomial curve. For each case study, the minimum BIC value was identified by considering polynomial degrees ranging from 1 to 5. The corresponding polynomial, with the minimum BIC value and the selected degree, was chosen to represent the curve  $m(C)$  accurately.

This approach ensures that the curve  $m(C)$  is represented by a polynomial equation of appropriate degree, striking a balance between the model complexity and its ability to capture the relationship between  $C$  and  $m$  accurately. Figure 7 illustrates that, in this specific example, the lowest BIC value is achieved with a polynomial degree of 5.

Figure 7 - Polynomial order that optimizes the BIC



Source: authors (2023)

As a result, the  $m(C)$  curve presented in Figure 7 can be accurately represented as:

$$m(C) = - 1.17x10^{51} * C^5 + 4.10x10^{41} * C^4 - 5.71x10^{31} * C^3 + 4.01x10^{21} * C^2 - 1.48x10^{11} * C + 5.02 \quad (2)$$

This equation will effectively represent the relationship between the physical parameters  $C$  and  $m$  for achieving the desired number of cycles  $n^*$ .

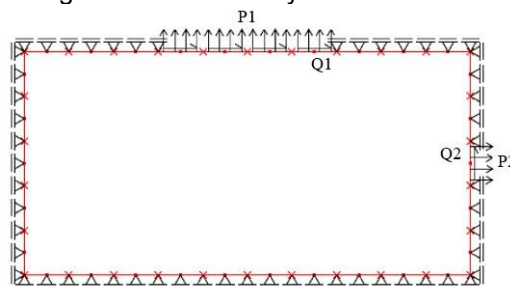
## 6 RESULTS AND DISCUSSIONS

To provide a demonstration of the technique's results, two case studies are presented. In each case study, a design engineer defines a Macro model by specifying different combinations of external loads and displacement constraint arrangements. The computational technique then processes the model and optimizes its fatigue life by employing the proposed methodology. By utilizing the technique, the design engineer can assess and enhance the fatigue life of the Macro model, taking into account the specified external loads and displacement constraints. The computational tool automates the process and provides optimized solutions for achieving the desired fatigue life for each case study.

### Case study 1

The Case Study 1 is presented in Figure 8. This model represents a fuselage piece subjected to normal (P) and shear (Q) external loads with values shown in Table 4 and with displacement restraint of degree 1 in the direction perpendicular to the other nodes.

Figure 8 – Case Study 1 Macro model.



Source: authors (2023)

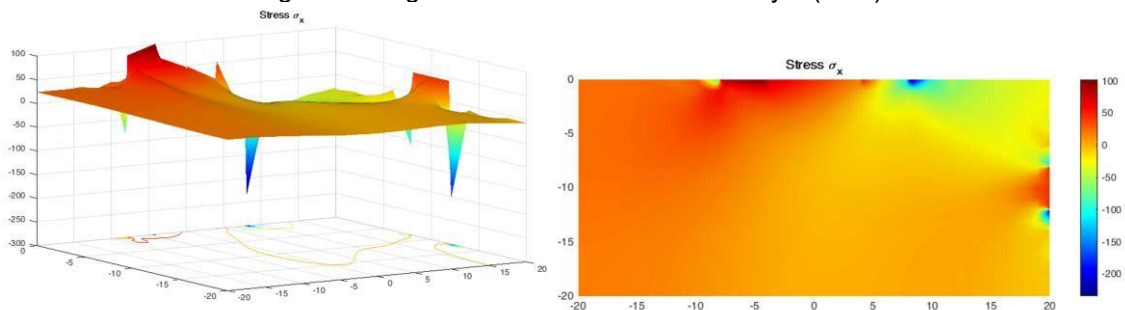
Table 4 - Case Study 1 variable values

Macro analysis variables	
P1 (MPa)	60.47
Q1 (MPa)	42.78
P2 (MPa)	43.58
Q2 (MPa)	90.70

Source: authors (2023)

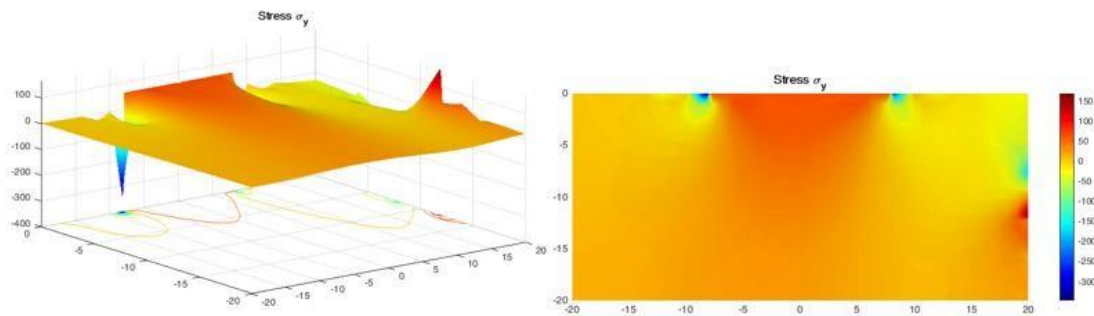
From the initial model, BemCracker2D calculates the internal stress fields of the macro model, as shown in Figures 9, 10 and 11, with the dimensions of the model highlighted on the x-y axes in meters.

Figure 8 – Sigma x stress field in Case Study 1 (MPa)



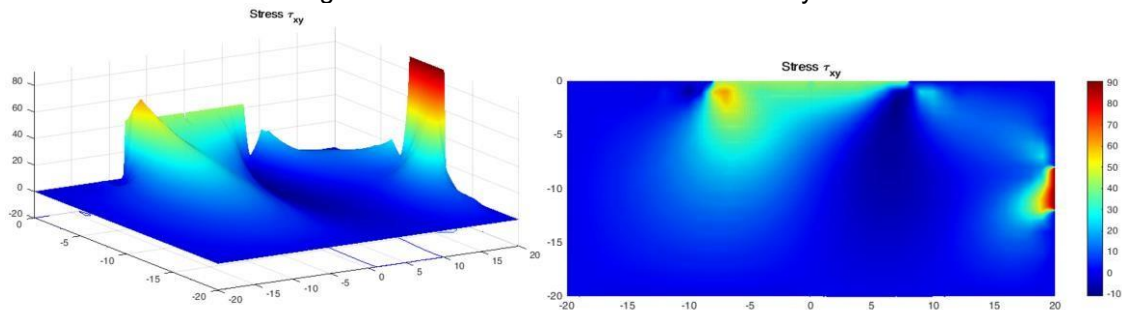
Source: authors (2023)

Figure 9 - Sigma y stress field in Case Study 1 (MPa)



Source: authors (2023)

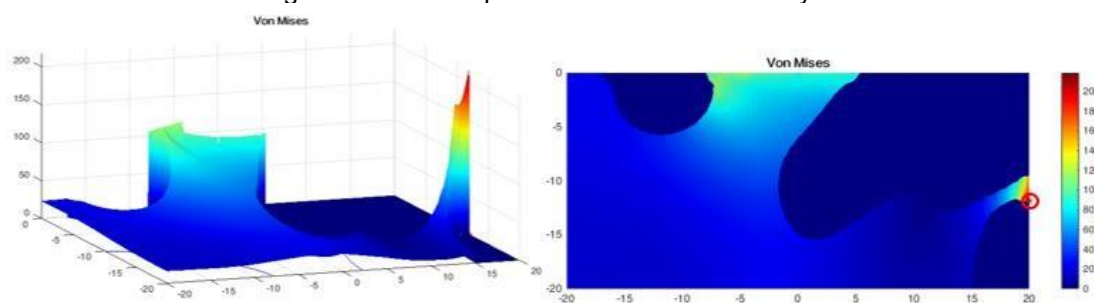
Figure 10 – Shear stress field in Case Study 1



Source: authors (2023)

Using the stress field, the critical stress location is analyzed using the von Mises criterion before reaching yielding, as shown in Figure 12.

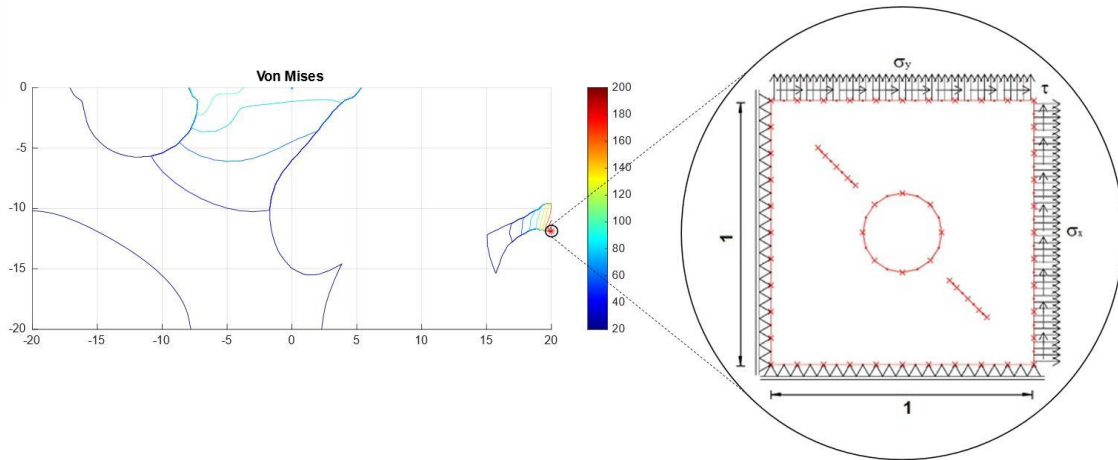
Figure 11 – Stress peak location in Case Study 1.



Source: authors (2023)

By identifying the location of the stress peak, the method positions the micro-element at this point and applies the internal stresses from this point, as shown in Figure 13. At this point, the values of the internal stresses are represented in Table 5.

Figure 12 - Positioning the Micro element in Case Study 1



Source: authors (2023)

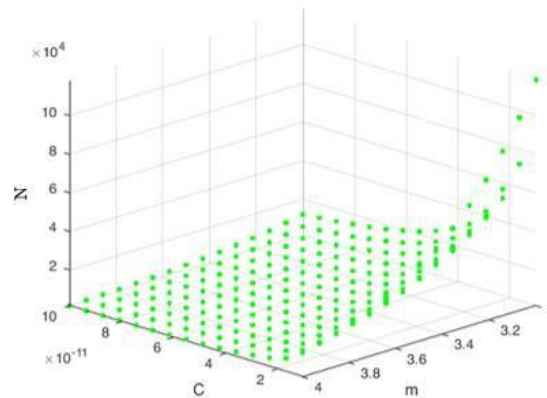
Table 5 - Stress values in Case Study 1

$\sigma_x$ (MPa)	43.58
$\sigma_y$ (MPa)	168.81
$\tau_{xy}$ (MPa)	90.70

Source: authors (2023)

The values of C and m of the Paris Law are varied, and the resulting number of fatigue cycles is calculated for each combination (C,m), as shown in Figure 14.

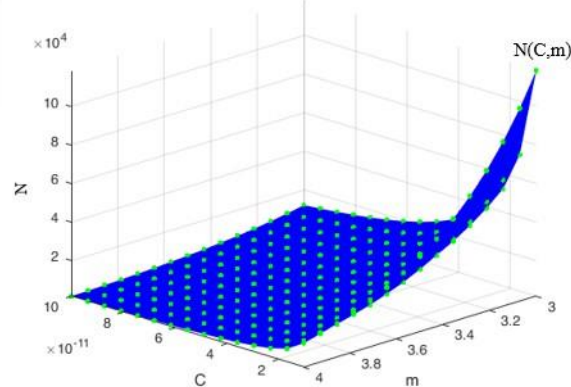
Figure 13 - Points of the number of cycles for each combination (C,m) in Case Study 1



Source: authors (2023)

The interpolation of these points results in the surface that relates the number of cycles to each combination (C,m), generating the function  $N(C,m)$ , as shown in Figure 15.

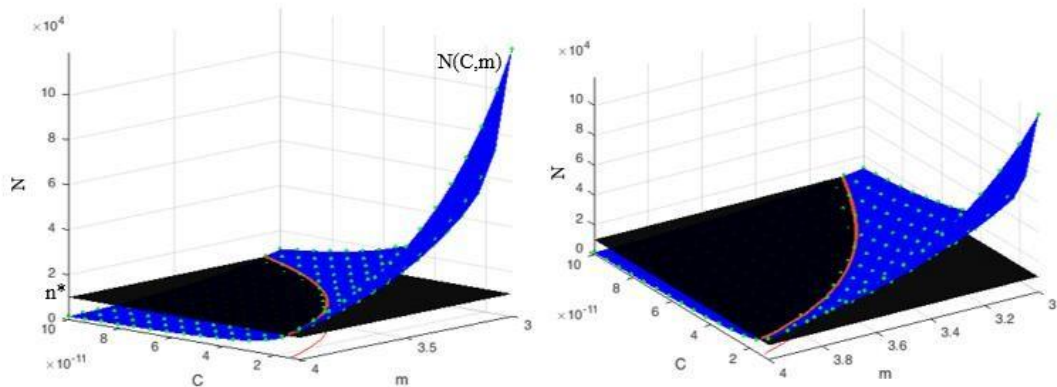
Figure 14 -  $N(C,m)$  surface in Case Study 1



Source: authors (2023)

Then, the method positions the number of project cycles ( $n^*$ ) defined by the designer, such that the intersection of  $N(C,m)$  with  $n^*$  results in the combination of C and m from the Paris Law for the required number of cycles in the project, as shown in Figure 16.

Figure 15 - Intersection of  $N(C,m)$  relation from Case Study 1 with the design number of cycles ( $n^*=10^4$ )

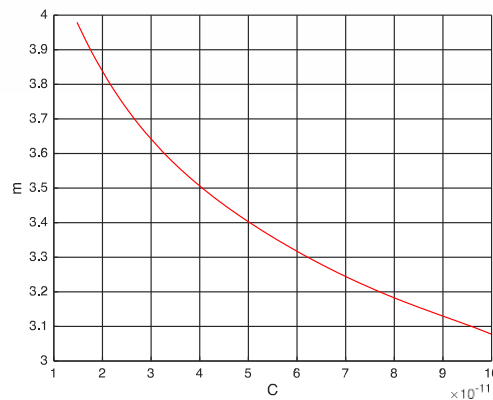


Source: authors (2023)

Thus, Figure 17 shows the combination of C and m from Paris Law for the number of cycles of  $10^4$ .



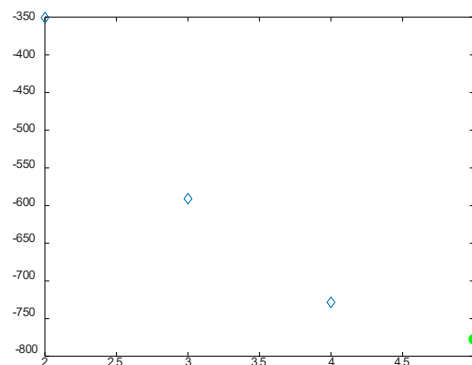
Figure 16 - Relationship  $m(C)$  that results in the design number of cycles  $10^4$



Source: authors (2023)

Finally, the curve equation is obtained through a polynomial regression with optimal degree defined by the BIC method. In this case, the polynomial with the lowest BIC was of degree 5, as shown in Figure 18.

Figure 17 - Degree of the polynomial that optimizes the BIC



Source: authors (2023)

As a result, the  $m(C)$  curve presented in Figure 17 can be accurately represented as:

$$m(C) = - 4.26x10^{50} * C^5 + 1.44x10^{41} * C^4 - 1.97x10^{31} * C^3 + 1.40x10^{21} * C^2 - 6.09x10^{10} * C + 4.63 \quad (3)$$

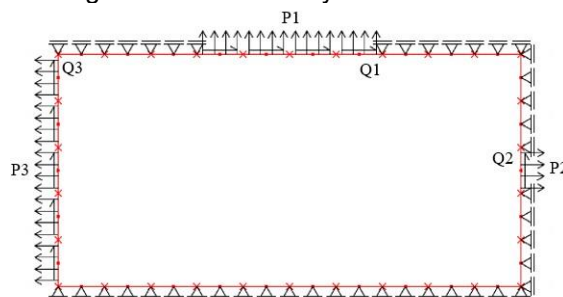
For Case Study 1, the combination of  $C$  and  $m$  from Paris Law for the number of cycles of  $10^4$  is represented in Equation (3). Therefore, the

computational technique provides the designer of Case Study 1 the physical parameters of the material that can withstand the required number of cycles in the project.

### Case study 2

Case Study 2 presents a similar model to Case Study 1 but adds normal (P3) and shear (Q3) stresses, as shown in Figure 19. Again, the values of each stress are presented in Table 6.

Figure 18 - Case Study 2 Macro model



Source: authors (2023)

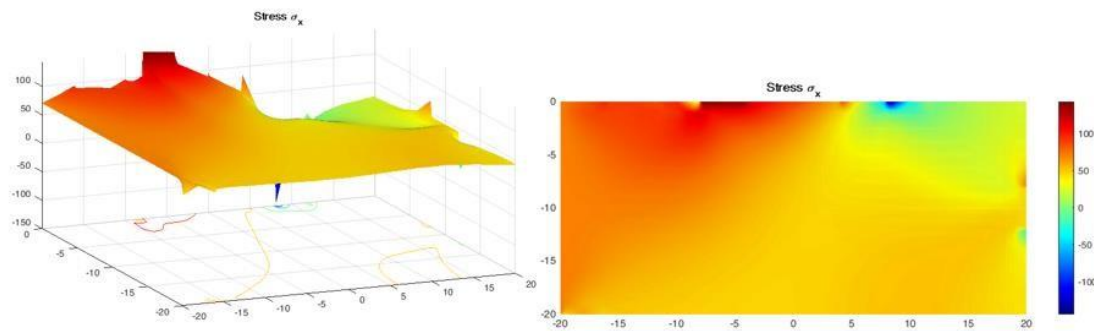
Table 6 - Case Study 2 variable values

Macro analysis variables	
P1 (MPa)	60.47
Q1 (MPa)	42.78
P2 (MPa)	43.58
Q2 (MPa)	90.70
P3 (MPa)	70.22
Q3 (MPa)	30.63

Source: authors (2023)

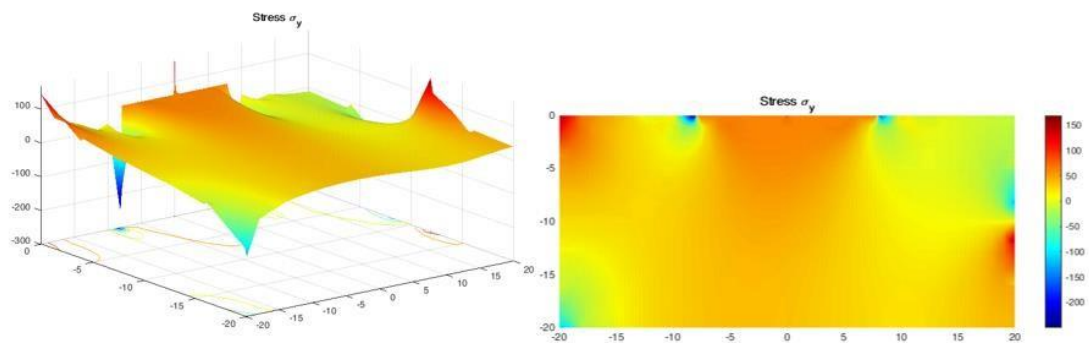
Based on the initial model, BemCracker calculates the internal stress fields of the macro model, as shown in Figures 20, 21 and 22, with the dimensions of the model highlighted in the x-y axes in meters.

Figure 19 – Sigma x stress field in Case Study 2 (MPa)



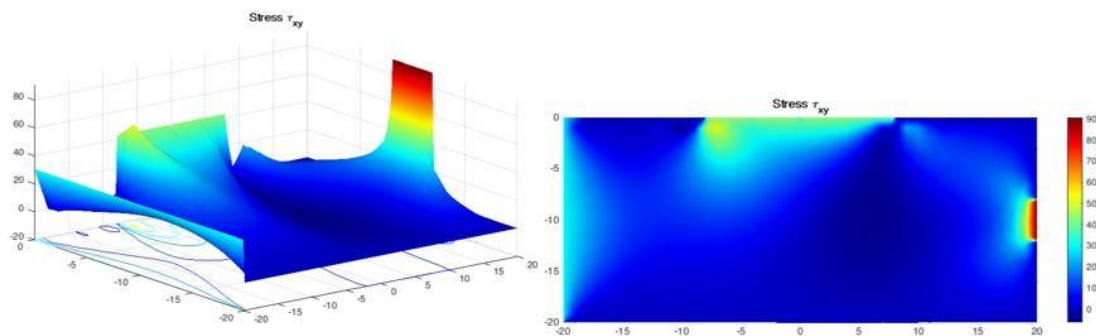
Source: authors (2023)

Figure 20 – Sigma y stress field in Case Study 2 (MPa)



Source: authors (2023)

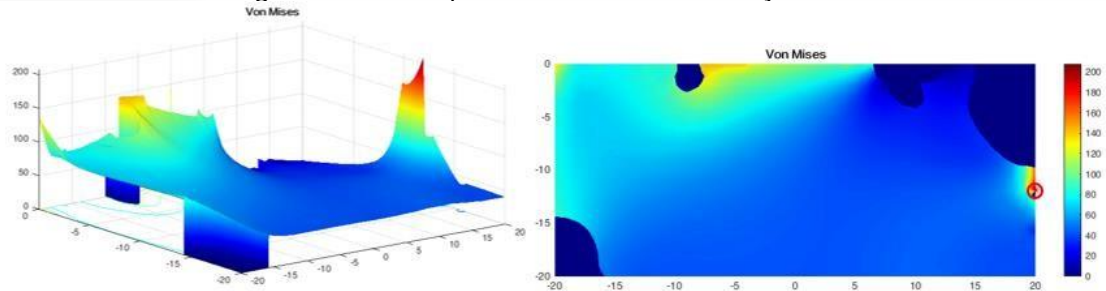
Figure 21 – Shear stress field in Case Study 2 (MPa)



Source: authors (2023)

With the stress field, the critical stress location is analyzed using the von Mises criterion before reaching yielding, as shown in Figure 23.

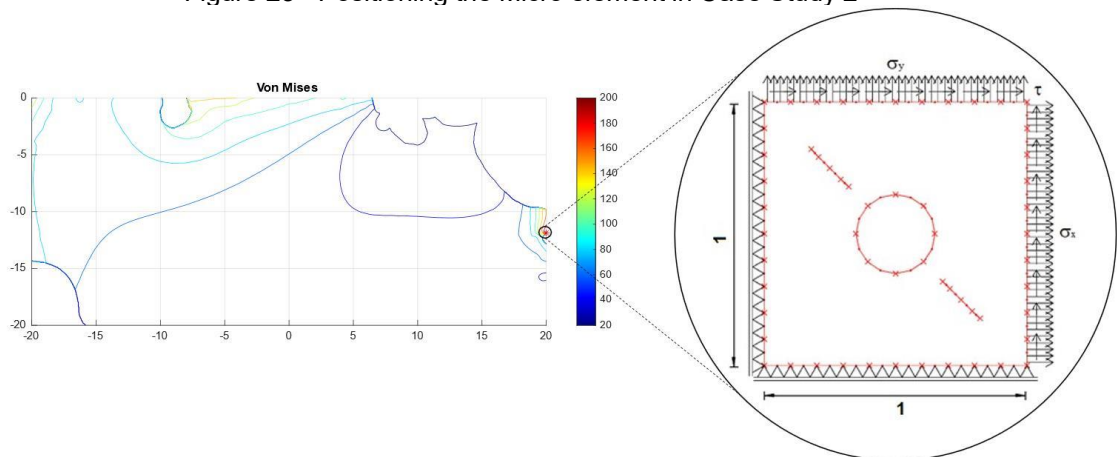
Figure 22 - Stress peak location in Case Study 2



Source: authors (2023)

Upon identifying the location of the stress peak, the method positions the microelement at this peak and applies the internal stresses at this point, as shown in Figure 24. At this point, the values of the internal stresses are represented in Table 7.

Figure 23 - Positioning the Micro element in Case Study 2



Source: authors (2023)

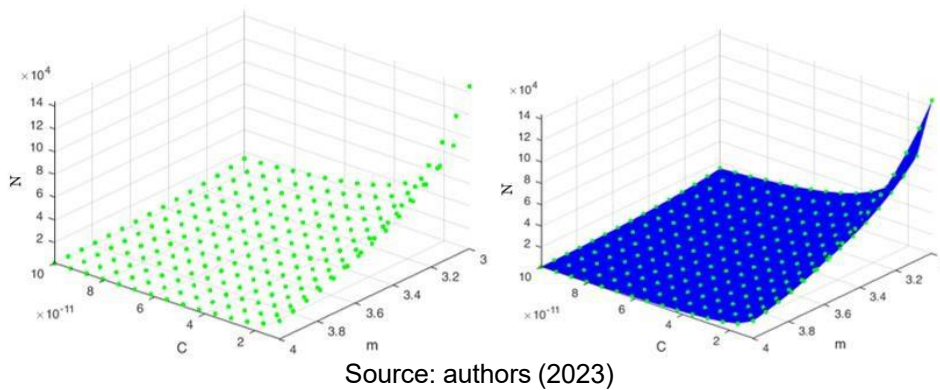
Table 7 - Stress values in Case Study 2

$\sigma_x$ (MPa)	43.58
$\sigma_y$ (MPa)	152.86
$\tau_{xy}$ (MPa)	90.70

Source: authors (2023)

It can be noticed that the stress values are similar to those of Case Study 1, since the critical point was the same, the only difference being the shear stress. Therefore, the values of  $C$  and  $m$  of the Paris Law are varied, and the resulting fatigue cycle count is calculated for each combination ( $C$ ,  $m$ ), as shown in Figure 25.

Figure 24 - Points of the number of cycles for each combination (C,m) in Case Study 2



The intersection of  $N(C,m)$  with  $n^*$  results in the combination of C and m from the Paris Law for the required number of cycles in the project, as seen in Figure 26.

Figure 25 - Intersection of  $N(C,m)$  relation from Case Study 2 with the design number of cycles ( $n^*=10^4$ )

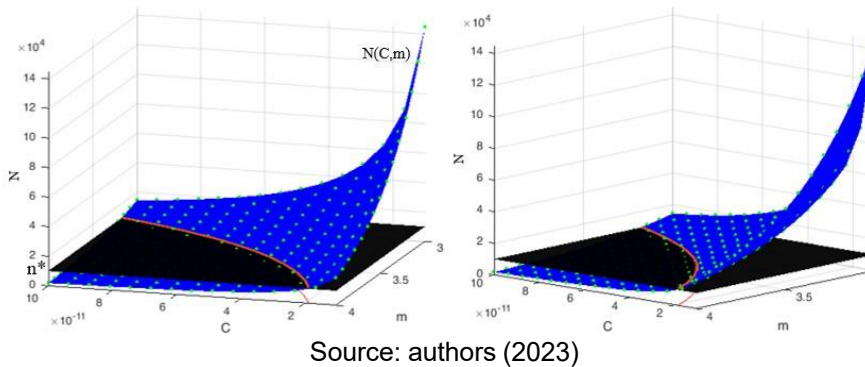
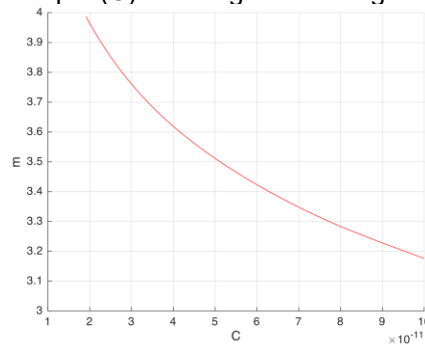


Figure 27 shows the combination of C and m for the number of cycles of  $10^4$ .

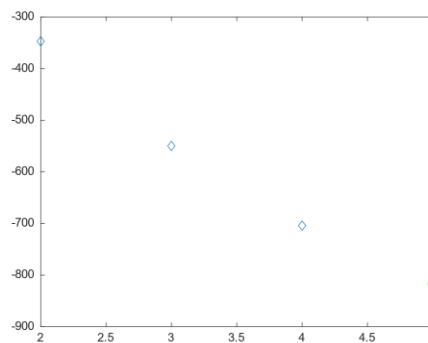
Figure 26 - Relationship  $m(C)$  resulting in the design number of cycles  $10^4$



Source: authors (2023)

Finally, the equation of the curve is obtained through a polynomial regression with optimal degree determined using BIC method. In this case, the polynomial with the lowest BIC was of degree 5, and the combination of C and m from Paris Law for the number of cycles of  $10^4$  is represented by Equation (4).

Figure 27 - Degree of the polynomial that optimizes the BIC



Source: authors (2023)

$$m(C) = - 3.52x10^{50} * C^5 + 1.24x10^{41} * C^4 - 1.76x10^{31} * C^3 + 1.31x10^{21} * C^2 - 5.98x10^{10} * C + 4.76 \quad (4)$$

## 7 FINAL REMARKS

In summary, the methodology presented in this study offers a valuable alternative to the conventional damage tolerance analysis approach, which typically revolves around critical crack size. Instead, this methodology focuses on evaluating compliance as a key factor for assessing instability.

The use of the Boundary Element Method (BEM) was crucial in the development of this technique. BEM's flexibility allowed for the evaluation of stress

peak locations and compliance at the edges of micro-analysis elements. This innovation has led to the establishment of a meaningful relationship between the Paris constants and the concept of damage tolerance, exemplified by the curve that correlates the Paris constants with the desired number of cycles.

The results clearly demonstrate that the  $N(C,m)$  curve is influenced by several factors, including model configuration, physical material parameters, and the specific number of cycles defined in the project. Consequently, for each model, there exists a range of  $C$  and  $m$  values that can fulfill the project requirements.

Moreover, the automation of the technique and the utilization of the Bem-Lab and BemCracker computational programs allow for the generalization of the approach to encompass any fuselage damage analysis model. The case studies presented in this study have showcased the effectiveness of this methodology, yielding valuable parametric data for the Paris constants and ensuring damage tolerance while preventing the structure from reaching a critical limit state.

In conclusion, this methodology offers a novel and comprehensive approach to damage tolerance analysis, departing from traditional crack size-based evaluations. It provides valuable insights for optimizing the fatigue life of aircraft fuselage structures, ultimately enhancing their safety and reliability.

## ACKNOWLEDGMENTS

The authors are grateful to the Brazilian Coordination for the Improvement of Higher Education (CAPES) for the supporting funds for this research. The authors also thank the Graduate Programme in Structural Engineering and Civil Construction in the Department of Civil and Environmental Engineering at the University of Brasilia, Brazil.

## REFERENCES

- [1] J. Ju and X. You, “Dynamic fracture analysis technique of aircraft fuselage containing damage subjected to blast,” *Math Comput Model*, vol. 58, no. 3–4, pp. 627–633, Aug. 2013, doi: 10.1016/j.mcm.2011.10.044.
- [2] A. Portela, M. H. Aliabadi, and D. P. Rooke, “The dual boundary element method: Effective implementation for crack problems,” *Int J Numer Methods Eng*, vol. 33, no. 6, pp. 1269–1287, Apr. 1992, doi: 10.1002/nme.1620330611.
- [3] A. Portela, M. H. Aliabadi, and D. P. Rooke, “Dual boundary element analysis of cracked plates: singularity subtraction technique,” *Int J Fract*, vol. 55, no. 1, pp. 17–28, May 1992, doi: 10.1007/BF00018030.
- [4] G. E. Blandford, A. R. Ingraffea, and J. A. Liggett, “Two-dimensional stress intensity factor computations using the boundary element method,” *Int J Numer Methods Eng*, vol. 17, no. 3, pp. 387–404, Mar. 1981, doi: 10.1002/nme.1620170308.
- [5] R. Citarella, “MSD crack propagation by DBEM on a repaired aeronautic panel,” *Advances in Engineering Software*, vol. 42, no. 10, pp. 887–901, Oct. 2011, doi: 10.1016/j.advengsoft.2011.02.014.
- [6] R. Citarella, P. Carlone, R. Sepe, and M. Lepore, “DBEM crack propagation in friction stir welded aluminum joints,” *Advances in Engineering Software*, vol. 101, pp. 50–59, Nov. 2016, doi: 10.1016/j.advengsoft.2015.12.002.
- [7] R. J. Price and J. Trevelyan, “Boundary element simulation of fatigue crack growth in multi-site damage,” *Eng Anal Bound Elem*, vol. 43, pp. 67–75, Jun. 2014, doi: 10.1016/j.enganabound.2014.03.002.
- [8] L. Morse, Z. S. Khodaei, and M. H. Aliabadi, “Multi-Fidelity Modeling-Based Structural Reliability Analysis with the Boundary Element Method,” *Journal of Multiscale Modelling*, vol. 08, no. 03n04, p. 1740001, Sep. 2017, doi: 10.1142/S1756973717400017.
- [9] X. Huang, M. H. Aliabadi, and Z. S. Khodaei, “Fatigue Crack Growth Reliability Analysis by Stochastic Boundary Element Method,” *CMES-Computer Modeling in Engineering & Sciences*, vol. 102, no. 4, pp. 291–330, 2014, doi: 10.3970/cmcs.2014.102.291.
- [10] G. Gomes and A. C. O. Miranda, “Analysis of crack growth problems using the object-oriented program bemcracker2D,” *Frattura ed Integrità Strutturale*, vol. 12, no. 45, pp. 67–85, Jun. 2018, doi: 10.3221/IGF-ESIS.45.06.
- [11] T. A. A. Oliveira, G. Gomes, and F. Evangelista Jr, “Multiscale aircraft fuselage fatigue analysis by the dual boundary element method,” *Eng Anal Bound Elem*, vol. 104, pp. 107–119, Jul. 2019, doi: 10.1016/j.enganabound.2019.03.032.



- [12] G. Gomes, T. Oliveira, and F. Evangelista Jr, “A Probabilistic Approach in Fuselage Damage Analysis via Boundary Element Method,” in *Advances in Fatigue and Fracture Testing and Modelling*, IntechOpen, 2022. doi: 10.5772/intechopen.98982.
- [13] G. Gomes, T. A. A. Oliveira, and A. M. Delgado Neto, “A new methodology to predict damage tolerance based on compliance via global-local analysis,” *Frat-tura ed Integrità Strutturale*, vol. 15, no. 58, pp. 211–230, Sep. 2021, doi: 10.3221/IGF-ESIS.58.16.
- [14] X. Ma, X. Liu, H. Wang, J. Tong, and X. Yang, “Fatigue Life Prediction of Half-Shaft Using the Strain-Life Method,” *Advances in Materials Science and Engineering*, vol. 2020, pp. 1–8, Aug. 2020, doi: 10.1155/2020/5129893.
- [15] M. Zhang, G. Hu, X. Liu, and X. Yang, “An improved strength degradation model for fatigue life prediction considering material characteristics,” *Journal of the Brazilian Society of Mechanical Sciences and Engineering*, vol. 43, no. 5, p. 275, May 2021, doi: 10.1007/s40430-021-02997-4.
- [16] X. Liu, J. Liu, H. Wang, and X. Yang, “Prediction and evaluation of fatigue life considering material parameters distribution characteristic,” *International Journal of Structural Integrity*, vol. 13, no. 2, pp. 309–326, Mar. 2022, doi: 10.1108/IJSI-11-2021-0118.
- [17] Y.-H. Li, C. Zhang, H. Yin, Y. Cao, and X. Bai, “Modification optimization-based fatigue life analysis and improvement of EMU gear,” *International Journal of Structural Integrity*, vol. 12, no. 5, pp. 760–772, Oct. 2021, doi: 10.1108/IJSI-07-2021-0072.
- [18] E. Breitbarth, T. Strohmann, and G. Requena, “High-stress fatigue crack propagation in thin AA2024-T3 sheet material,” *Fatigue Fract Eng Mater Struct*, vol. 43, no. 11, pp. 2683–2693, Nov. 2020, doi: 10.1111/ffe.13335.
- [19] P. M. Toor, “On damage tolerance design of fuselage structure (longitudinal cracks),” *Eng Fract Mech*, vol. 24, no. 6, pp. 915–927, Jan. 1986, doi: 10.1016/0013-7944(86)90276-6.
- [20] P. M. Toor, “On damage tolerance design of fuselage structure—circumferential cracks,” *Eng Fract Mech*, vol. 26, no. 5, pp. 771–782, Jan. 1987, doi: 10.1016/0013-7944(87)90140-8.
- [21] B. Sayar and A. Kayran, “Two-stage fatigue life evaluation of an aircraft fuselage panel with a bulging circumferential crack and a broken stringer,” *Fatigue Fract Eng Mater Struct*, vol. 37, no. 5, pp. 494–507, May 2014, doi: 10.1111/ffe.12127.
- [22] J. G. Bakuckas et al., “Assessment of emerging metallic structures technologies through test and analysis of fuselage structure,” *SN Appl Sci*, vol. 1, no. 11, p. 1521, Nov. 2019, doi: 10.1007/s42452-019-1471-7.

- [23] F. Abdi, Y. Xue, M. Garg, B. Farahmand, J. Housner, and K. Nikbin, “An analysis approach toward FAA certification for damage tolerance of aircraft components,” *The Aeronautical Journal*, vol. 118, no. 1200, pp. 181–196, Feb. 2014, doi: 10.1017/S0001924000009064.
- [24] F. Carta and A. Pironi, “Damage tolerance analysis of aircraft reinforced panels,” *Frattura ed Integrità Strutturale*, vol. 5, no. 16, pp. 34–42, Apr. 2011, doi: 10.3221/IGF-ESIS.16.04.
- [25] C. Proppe, “Probabilistic analysis of multi-site damage in aircraft fuselages,” *Comput Mech*, vol. 30, no. 4, pp. 323–329, Mar. 2003, doi: 10.1007/s00466-002-0408-x.
- [26] T. C. Kennedy, M. H. Cho, and M. E. Kassner, “Predicting failure of composite structures containing cracks,” *Compos Part A Appl Sci Manuf*, vol. 33, no. 4, pp. 583–588, Apr. 2002, doi: 10.1016/S1359-835X(01)00145-2.
- [27] N. Madhavi and R. Saritha, “Two bay crack arrest capability evaluation for metallic fuselage,” *IOP Conf Ser Mater Sci Eng*, vol. 455, no. 1, p. 012015, Dec. 2018, doi: 10.1088/1757-899X/455/1/012015.